# Role of the dew water on the ground surface in HONO distribution: a case measurement in Melpitz

**Yangang Ren[1], Bastian Stieger[2], Gerald Spindler[2], Benoit Grosselin[1], Abdelwahid Mellouki[1*], Thomas Tuch[2], Alfred Wiedensohler[2], Hartmut Herrmann[2*],**

1. Institut de Combustion, Aérothermique, Réactivité et Environnement (ICARE), CNRS (UPR 3021), Observatoire des Sciences de l'Univers en région Centre (OSUC), 1C Avenue de la Recherche Scientifique, 45071 Orléans Cedex 2, France

2. Leibniz Institute for Tropospheric Research (TROPOS), Permoserstraße 15, 04318 Leipzig, Germany

* Corresponding author: Abdelwahid Mellouki (abdelwahid.mellouki@cnrs-orleans.fr) and Hartmut Herrmann (herrmann@tropos.de)

## Supplement

**Table S1**. The reactions exist regarding on the HONO formation and loss in the atmosphere and OH formation from $O_3$ photolysis.

| **HONO sink** | **Number in the text** |
|---|---|
| HONO + hν → OH + NO | (1) |
| HONO + OH → $H_2O$ + $NO_2$ | (10) |
| **HONO source** | **Number in the text** |
| $2NO_2$ + $H_2O$ → HONO + $HNO_3$ | (2) |
| $2NO_2$ (g) ↔ $N_2O_4$ (g) ↔ $N_2O_4$ (surface) ↔ HONO (surface) + $HNO_3$ (surface) | (2a) |
| $NO_2$ +$\{C-H\}_{red}$ → HONO + $\{C\}_{ox}$ | (2b) |
| $NO_2$ (ads) + H (ads) → HONO (ads) → HONO (g) | (2c) |
| NO + OH → HONO | (3) |
| NO + $NO_2$ + $H_2O$ → 2HONO | (4) |
| $NO_2$ (g) + $H_2O$ (g) + $NH_3$ (g) → HONO (g) + $NH_4NO_3$ (s) | (5) |
| $NO_2$ + hν → $NO_2$* $NO_2$* + $H_2O$ → HONO + OH | (6) |
| NO + $HNO_3$ (surface) → HONO + $NO_2$ | (7) |
| $HNO_3/NO_3^-$ + hν → HONO/$NO_2^-$ + O | (8) |
| $NO_2^-$ (aq) + $H^+$ (aq) → HONO (aq) | (9) |
| **OH formation from $O_3$ photolysis** | |
| $O_3$ + *hυ* → $O(^1D)$ + $O_2$ (λ <320 nm) | (11) |
| $O(^1D)$ + $H_2O$ → 2OH | (12) |
| $O(^1D)$ + M → $O(^3P)$ + M (M =$N_2$) | (13) |

**Figure S1a**

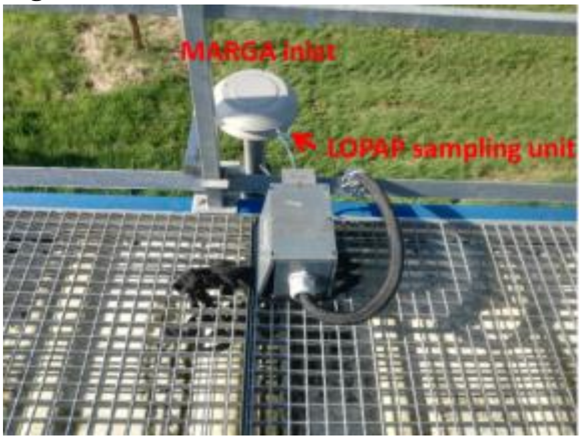


**Figure S1b**

**Figure S1a**. M1; sampling unit of LOPAP was connected in front of the WRD and in the back of the 2 m sampling inlet of MARGA (18 April 2018 13:00 UTC – 20 April 2018 08:00 UTC).
**Figure S1b:** M2; sampling unit of LOPAP was settled in the same level as the sampling head of MARGA (20 April 2018 15:00 UTC – 29 April 2018 07:00 UTC).

**Figure S2**. The dew collector system: The glass sampler surface is 1.0×1.5 $m^2$, and about 40 cm above ground at the lowest point.

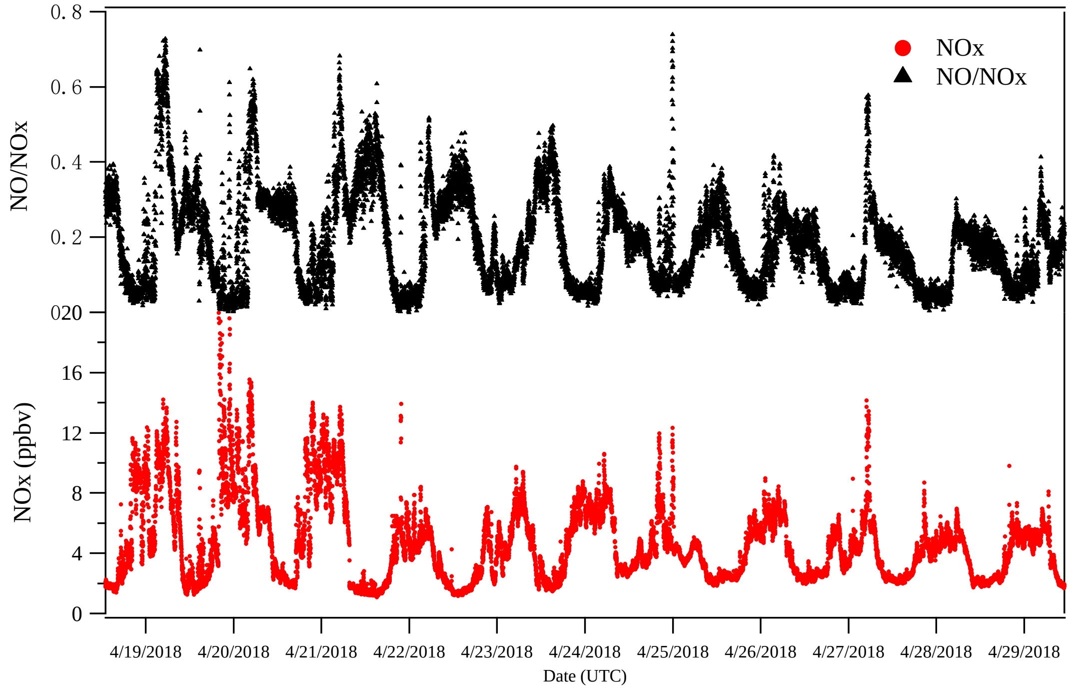


**Figure S3**. Time profile of $NO_x$ and $NO/NO_x$ from 19 to 29 April 2018.

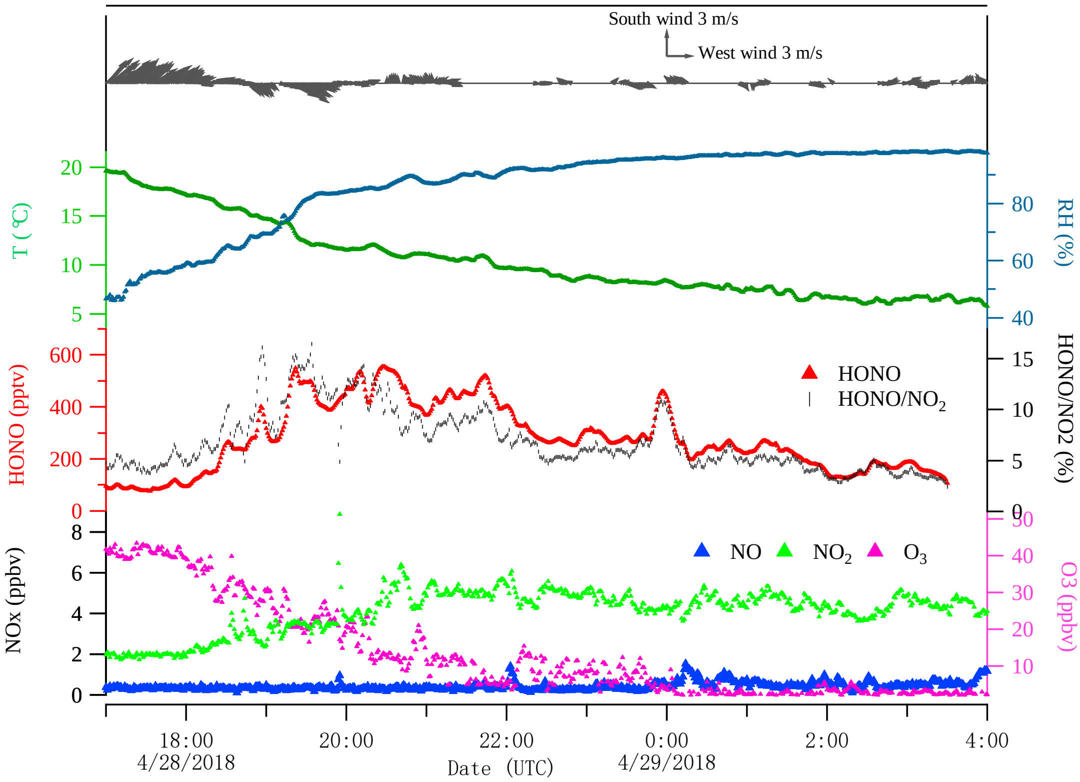


**Figure S4.** A case of the determination of the heterogeneous $NO_2$-to-HONO conversion frequency at night from 28 April until 29 April 2018.

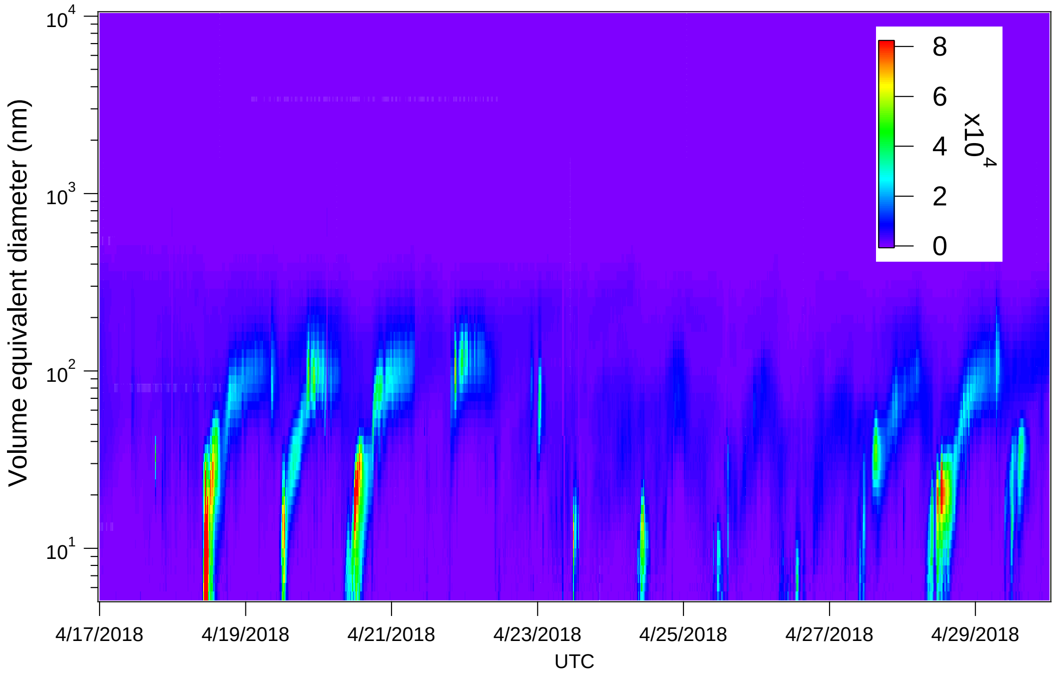


**Figure S5**. Particle size distribution ranged from 5 nm to 10 μm of APSS and D-MPSS data. The mobility diameter is to be assumed to be identical to the volume equivalent diameter due to compact particles

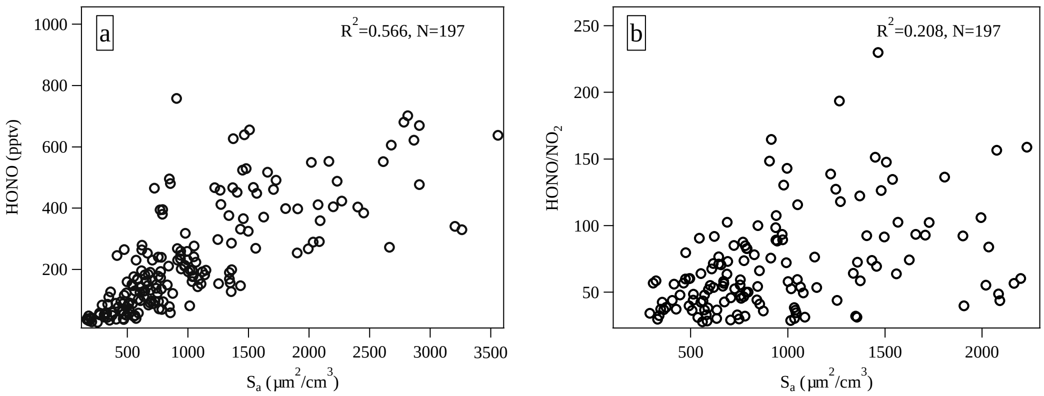


**Figure S6.** Correlation between (a) $HONO/NO_2$ and (b) HONO with particle surface density during the time interval of 17:30-22:00 (UTC)

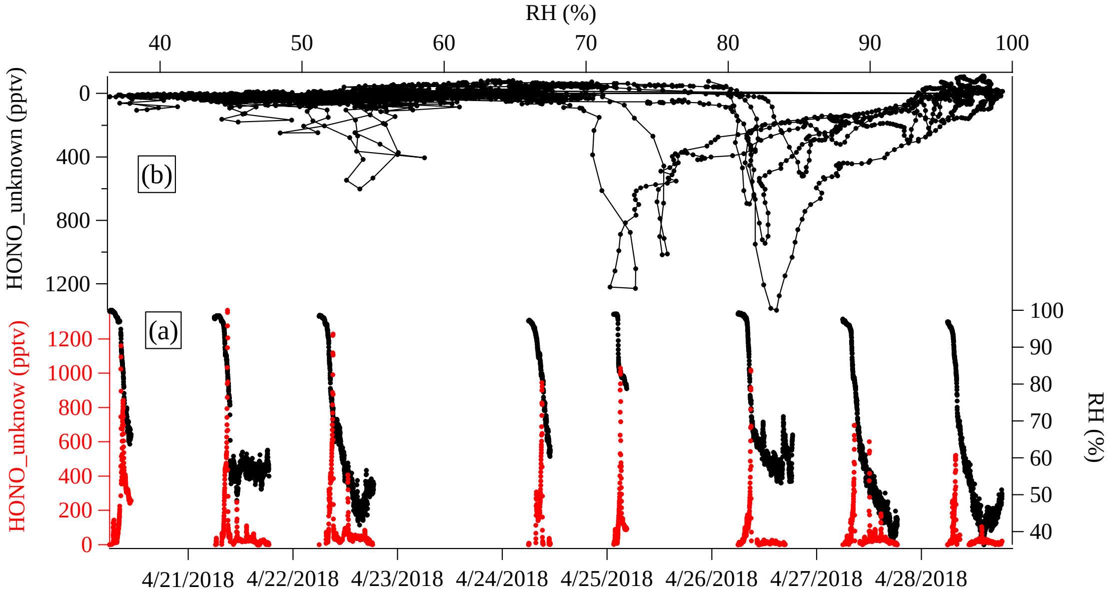


**Figure S7.** (a) Time-profile of HONO and RH; (b) the HONO_unknown as a function of RH (%) during daytime in the period of 20 to 29 April 2018; HONO_unknown was obtained by subtracting modeled HONO (HONO_Model4) from the measured HONO.

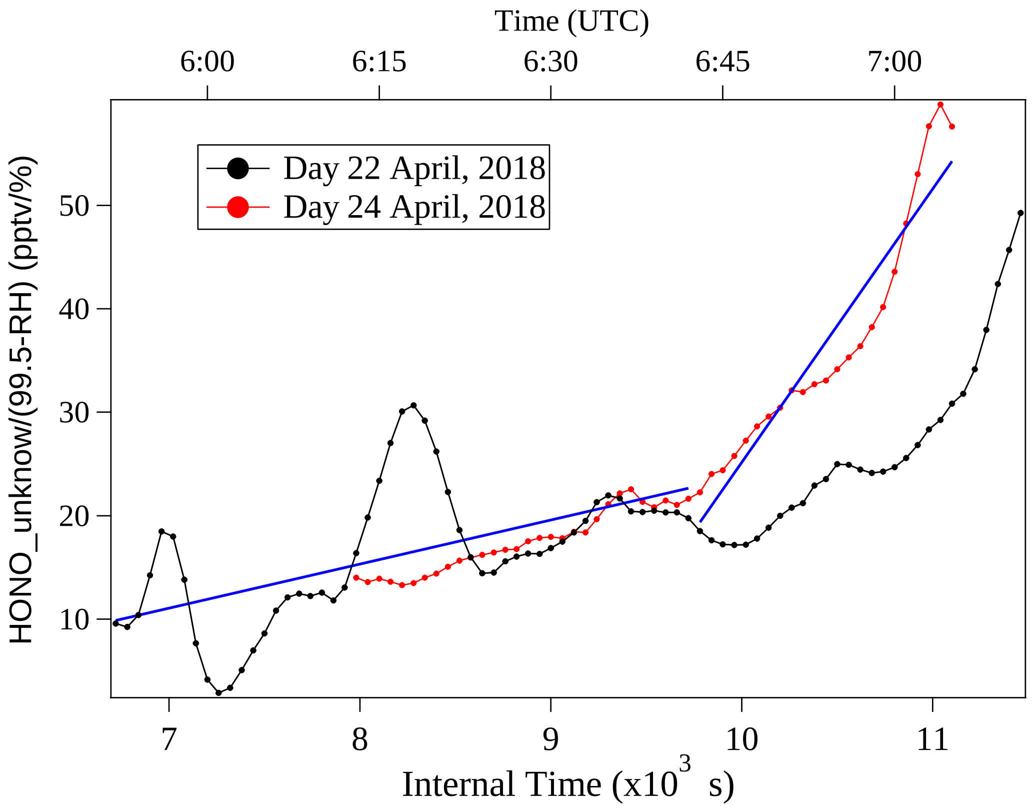


**Figure S8.** Example of $\frac{HONO_{unknown}}{99.5-RH}$ as a function of the internal time of HONO morning peak (zero point from time 4:30, UTC) to estimate the temporary HONO emission rate from dew water, $k_{emission}$. Blue line is the linear least-square analysis of $\frac{HONO_{unknown}}{99.5-RH}$ vs. internal time to obtain the minimum and maximum of $k_{emission}$, respectively.

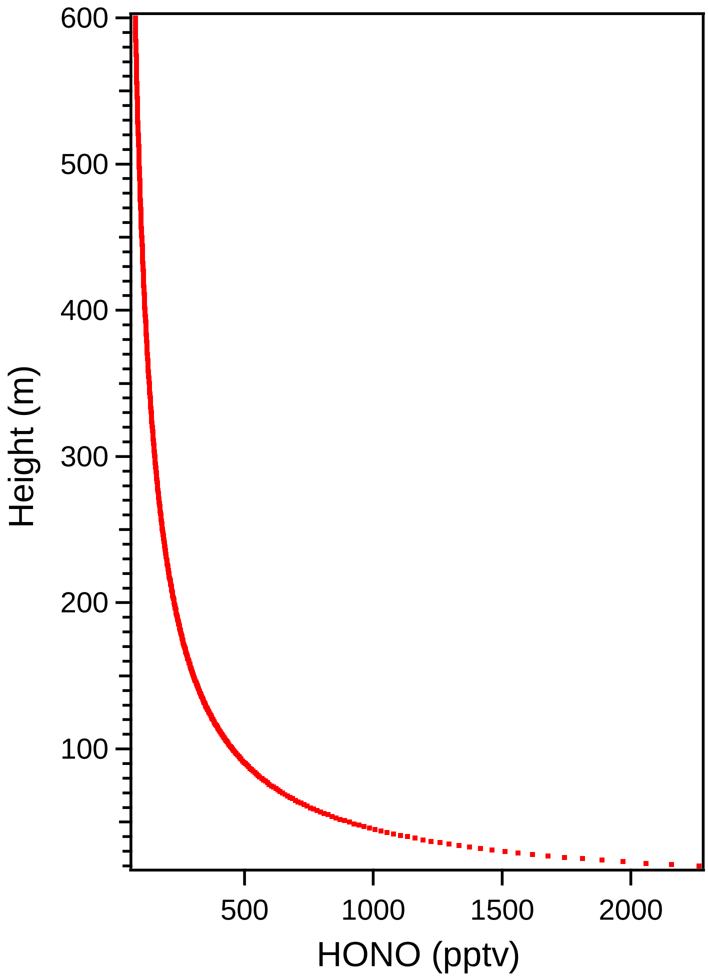


**Figure S9.** Evolution of HONO vertical profiles presented in the Melpitz station on 8-14 May 2019 from 5:00 to 07:00 UTC.